AIAA Aviation
16-20 June 2014, Atlanta, GA
15th AIAA/ISSMO Multidisciplinary Analysis and Optimization Conference

Reducing Spacecraft Jitter During Satellite Reorientation Maneuvers via Solar Array Dynamics

Daniel R. Herber*, Jason W. McDonald†,
University of Illinois at Urbana-Champaign, Urbana, IL, 61801, USA
Oscar S. Alvarez-Salazar‡,
Jet Propulsion Laboratory, Pasadena, CA, 91109, USA
Girish Krishnan§ and James T. Allison¶
University of Illinois at Urbana-Champaign, Urbana, IL, 61801, USA

Jitter and excessive settling time after slewing maneuvers has proven to be a severe limitation on the scientific utility of a number of spacecraft. In this article a new design and control strategy is presented that is based on advanced solar arrays that exploit their inertial properties and a balance of passive and active dynamics to minimize jitter and settling time, thereby boosting spacecraft scientific utility. This development will require the advancement of some promising optimization-based methods for simultaneous physical and control system design to determine the best possible synergy between the control system and passive structural system dynamics. The solar array will be designed specifically to be compliant using pseudo-rigid-body dynamic modeling theory. Shooting will be utilized to solve the optimal control problem posed in the co-design formulation.

I. Introduction

Attitude control of satellites and other space structures is a common design concern since many components need to be directed towards a particular reference point. For example, solar arrays (SAs) need to be oriented towards the Sun, while cameras need to track a celestial body. While performing its primary function, satellites encounter an unwanted phenomenon known as jitter. These are disturbance vibrations in spacecraft caused by a number of sources including reaction wheels, control moment gyroscopes, solar drive motors, thruster rings, cryogenic coolers, gimbaled instruments, and slew maneuvers (i.e., change of orientation). Most satellites require a hybrid system of passive and active elements to suppress the entire range of disturbance frequencies.[1]

The vibration and attitude control problems are commonly explored separately. The SA may be designed by the mechanical engineers to satisfy mass, frequency, and stress constraints. Then the structural design of the array is provided to the control engineers who then strive to develop a control system that can perform reorientation maneuvers with the given design while meeting a range of requirements.[2] If the SA is unsuitable for the slewing maneuver, the structural and control engineers iterate between designs. While this iterative strategy may lead to an acceptable design, it is often inefficient and can have convergence issues, wasting large numbers of man-hours.[3,4] Since the maneuver itself can produce unwanted disturbances in the scientific equipment, considering both the problems during the design of the system are critical for maintaining high scientific utility of the spacecraft.

*Graduate Student, Department of Industrial and Enterprise Systems Engineering, 104 S. Mathews Ave, Urbana, IL, 61801, AIAA Student Member
†Graduate Student, Department of Industrial and Enterprise Systems Engineering, 104 S. Mathews Ave, Urbana, IL, 61801, AIAA Student Member
‡Supervisor G&C Systems Engineering Group, 4800 Oak Grove Dr, Pasadena, CA, 91109
§Assistant Professor, Department of Industrial and Enterprise Systems Engineering, 104 S. Mathews Ave, Urbana, IL, 61801
¶Assistant Professor, Department of Industrial and Enterprise Systems Engineering, 104 S. Mathews Ave, Urbana, IL, 61801, AIAA Member

Conventional requirements for SA design include low mass, power generation, deployability, and structural integrity (both during launch and during operation). The mass constraint leads to highly flexible, elastically compliant SAs. In addition, the panels are traditionally isolated from the other control systems to decouple their dynamic behavior as much as possible. Since this large amount of distributed mass is already being flown on the spacecraft, NASA is interested in secondary functions it may perform during the mission. In this article, we will investigate the use of the SA as the critical passive/active element of the system to suppress jitter by controlling its structural properties while still performing its primary functions.

Many classical problems in attitude control use dynamic equations that are limited to rigid-body motion.[5] However, the drive to decrease overall mass and reduce the number of mechanical interfaces or joints has led to utilization of structural flexibility or mechanical compliance in space structures.[6] This includes work on flexible antennas,[7,8] flexible solar panels,[9] and general robust control of flexible space structures.[6] Components do not need to be large to be considered flexible; even more commonly sized components such as a solar panel can be designed to have low stiffness.

Compliant system research has typically focused on models that facilitate elastostatic and kinematic analysis and synthesis.[10] Similarly, models that capture the dynamic behavior of compliant systems that facilitate their design synthesis for a desired dynamic behavior will greatly benefit the goal of simultaneous passive system and control system design. One such method frequently used to model flexible planar robot dynamics is based on incorporating a nonlinear finite element formulation that captures the effects of large deformation kinematics.[11,12] However, this approach might be computationally expensive, especially when coupled with an optimal control problem. A computationally inexpensive alternative involves the use of a pseudo-rigid body model (PRBM) where a compliant segment is modeled as a rigid link with a torsional spring at its joint.[13] This decoupling of its kinematic and elastic behavior renders PRBM to be more suitable for design. Yu et al. extended PRBM theory to dynamic systems known as pseudo-rigid-body dynamic models (PRBDMs).[10] Designing the parameters of the PRBDMs is a first step towards obtaining a conceptual design of the structural system.

While many studies have addressed the challenges associated with designing a control system for a flexible structure, most consider the controller design problem only.[7,8,9] Combining physical and control system design (co-design) has been shown to achieve the optimal balance of passive dynamics and active control to minimize system-level objectives while satisfying other requirements[4] (i.e., a system-optimal design). Many authors have noted the tight integration of the structure and control in large space structures, motivating co-design formulations.[2,3,8,14] Sunar and Rao explored a hybrid system with flexible appendages modeled by a spring/mass system. Their co-design formulation designed the passive control through structural modifications and the active control with negative state feedback.[15] Frequency domain strategies are often used when attempting to solving the jitter reduction problem, but this approach cannot address the large-angle slewing maneuver.[14] Therefore, a co-design approach in the time domain is necessary for a successful design of a compliant satellite.

An important element of any co-design strategy is a practical method of solving the associated optimal control problem. Direct methods of optimal control first discretize the problem and then transcribe it to a nonlinear program (NLP), whereas indirect methods, such as those based on Pontryagin's maximum principle, utilize the reverse process.[4] In other words, an infinite-dimensional optimal control problem is transcribed to a finite-dimensional NLP when direct methods are used.[16] Shooting is a particular direct method where the control trajectory is parameterized with a number of optimization variables. Direct methods has also been found to be particularly useful when the controller design needs to be unrestricted; for example, at early stages of the design process it is beneficial to accommodate arbitrary control trajectories without making assumptions about control system architecture.[17] This permits exploration of system performance limits, and the resulting trajectories can provide insights into the type of feedback control architecture that may be appropriate.[18] Some investigators have identified that value using an unrestricted control formulation specifically for spacecraft design problems.[19] A common control architecture used in the literature is a linear-quadratic regulator.[3,14] These control structures may be closer to the final control design, but are fundamentally limited in the control trajectories that they can generate, and may not produce the ideal system performance.[8] An unrestricted control trajectory design approach will be used here.

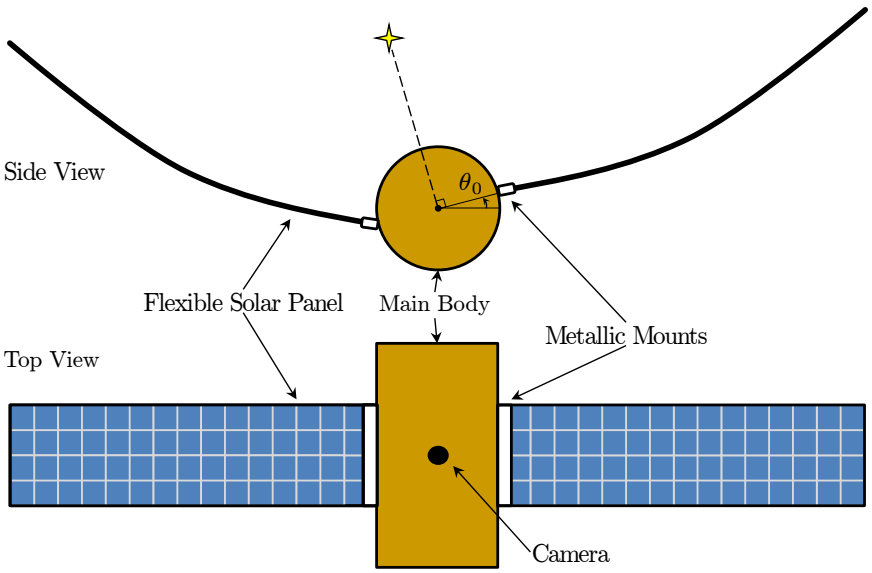

Figure 1: Side and top diagram of satellite with camera and flexible solar arrays.

II. System Model with Flexible Solar Arrays

Models for the attitude control of a three-axis stabilized spacecraft often treat the spacecraft as a rigid body.[5] In this case the dynamics and kinematics of the system can be represented easily using Newton-Euler equations. In a flexible system, however, the calculated moments of inertia may change depending on system state, especially for large deformations. Perhaps more importantly, modeling the system as rigid surrenders the ability to exploit system flexibility and consider important design constraints.

Several simplifying assumptions are made here for this initial study, while still accounting for the dynamics of the flexible system. Future work will involve the development of increasingly high-fidelity models, and their use in spacecraft (SC) co-design. Incorporating high-fidelity models into co-design is a significant challenge that so far has only begun to be addressed. Initial advancements in using high-fidelity models for co-design have involved the use of adaptive surrogate modeling for the time derivative function in a state-space model (instead of a surrogate model based on simulation responses). This approach has been validated using a wind turbine co-design case study that involved high-fidelity aeroelastic analysis.[20]

The initial studies here will be performed in an internal reference frame where the orbital dynamics are ignored. Additionally, only symmetric moments about the z-axis will be applied to the satellite (i.e., the moment functions along the left and right panels in Fig. 1 are identical). With these assumptions, the line of sight attitude will be fixed during the problem's time horizon, and the center of the satellite body (SB) will remain stationary in the local xy frame. This formulation is not valid for many space systems, but is important in stellar interferometers, large monolithic space telescopes, and large segmented space telescopes. An external reference frame and its associated dynamics maybe added depending on the goals of the satellite.[5,19]

A conceptual picture of the satellite with exaggerated flexible solar panels can be seen in Fig. 1. In our problem formulation, the camera is oriented 90° from the SB. The SA is single-sided and cantilevered from the SB using a metallic mount interface. The natural bending frequency is 2.5 Hz. The elastic modulus will be selected to yield the correct frequency. The SA is modeled as a homogeneous rectangular prism with a mass of 20 kg, $\ell = 2$ m along the x-axis, $w = 1.5$ m along the z-axis, and a thickness of $h = 0.025$ m along the y-axis. The SB is a cylinder at the origin with a mass of 1000 kg and radius of 1 m. However the inertia is set as $I_{zz} = 2000$ kgm^2. Two metallic mounts connect the SB to the SA panel at the corners of the panel closest to the SC. These mounts will be modeled as springs with a finite stiffness determined by the previously defined structural modes.

II.A. Internal vs. External Actuation Models

The SC described here aims to utilize SA actuation to perform both slew maneuvers and to reduce jitter. This type of actuation can be realized through embedding components such as piezoelectric actuators within the SA structure to produce internal moments. If no external forces act on the system (e.g., thrusters, interaction with Earth's magnetic field, etc.), angular momentum must be conserved. In other words, internal actuators cannot change the total angular momentum of the system. This places significant limitations on what maneuvers can be performed using SA actuation. It is possible to change SB orientation by moving the solar arrays, but there are limits on the magnitude of this orientation change. Figure 2 illustrates a very simplified model of a SC that will help illustrate these issues.

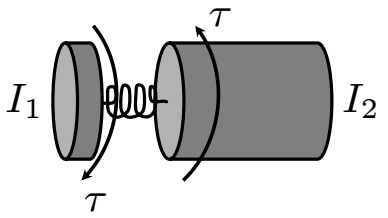

$$I_1\alpha_1 = \tau + k\left(\theta_1 - \theta_2\right) + b\left(\dot{\theta}_1 - \dot{\theta}_2\right)$$
$$I_2\alpha_2 = -\tau - k\left(\theta_1 - \theta_2\right) - b\left(\dot{\theta}_1 - \dot{\theta}_2\right)$$

Figure 2: SC conceptualization for momentum considerations.

This model involves two inertias that can rotate about a common axis. The larger inertia, I_2, is analogous to the SB, and the smaller inertia, I_1, is analogous to the SA if we assume that the arrays rotate with respect to the SB as a single rigid unit. It is assumed here that a servo connects the two inertias, and can exert an internal torque τ between them. The SA and SB are connected mechanically via an elastic element with some damping, and the equations of motion are shown in the figure.

In this model, no external forces can be applied to the system. If the system starts at rest (i.e., $\omega_1 = \omega_2 = 0$), the total system momentum must remain zero for any internal actuator moment trajectory (i.e., $p_T = p_1 + p_2 = I_1\omega_1 + I_2\omega_2 = 0 \quad \forall t$). We could use the servo to rotate the inertias relative to each other to change the position of the SB to a desired position. At the end of the maneuver we would need to trail off the control moment so that the SB at the final time achieves the desired orientation with zero rotational velocity for both components. This also requires that we hold the SA in its deformed position. Any attempt to move it back to an undeformed position will cause the SB to deviate from the desired orientation. Additional mechanisms (e.g., mechanical releases, coordination with a reaction wheel or external actuation), would be required to bring the SA back to its original position relative to the SB without disturbing the SB orientation.

If there was no limit on how far the SA could be displaced, we could orient the SB in any arbitrary position. Since the SA inertia is typically much smaller than the SB inertia, rotating the SB to a particular position requires a much larger rotation of the SA. In other words, $|\theta_1| \gg |\theta_2|$. To rotate the SB by π radians, several revolutions of the SA would be required. In an actual spacecraft, there is a limit to how far the array can rotate, placing an inherent limit on the range of slew maneuvers that can be achieved via SA actuation.

The conceptual model described above illustrates potential SC behavior based on internal SA actuation. For modeling convenience at the early stage of this investigation, an alternative strategy was used. As described in the following subsections, it is assumed that moments applied to bodies in the pseudo-rigid body models are applied with respect to an inertial reference frame (i.e., external actuation). The results for slewing maneuvers only approximate what would occur with internal actuation, but provide important insights into system dynamics. Ongoing work is addressing models that utilize internal actuation, and these models will support investigations that will establish design limitations and tradeoffs that are inherent to internal SA actuation.

II.B. Pseudo-Rigid-Body Dynamics

PRBMs link the motion and force of an elastic member and a rigid-body mechanism through a set of diagrams and equations that describe this correspondence. The main advantage of PRBMs is an accurate simplification of large-deflection nonlinear analysis of beams.[10] However, these models only describe the behavior at a component level rather than the specific point-to-point variations.[13] With 99.5% accuracy, the flexible beam of length ℓ in Fig. 3a can be approximated by the rigid model and spring in Fig. 3b when

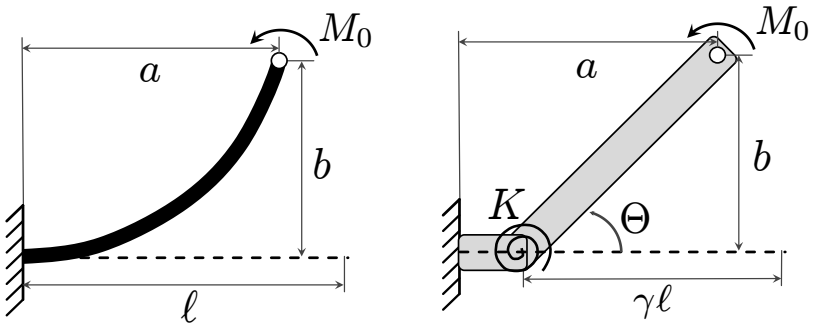

(a) Original flexible beam. **(b) Pseudo-rigid-body model.**

Figure 3: Pseudo-rigid-body model of a cantilever beam with an applied moment at the free end.

subjected to an end moment M_0. The spring constant in Fig. 3b can be calculated by:

$$K = \gamma K_\theta \frac{EI}{\ell} \tag{1}$$

where γ is the characteristic radius factor, K_θ is the stiffness coefficient, I is the area moment of inertia, and E is the Young's modulus. The distance between the spring and end moment is $\gamma\ell$. A linear fit can be found between the beam end angle, θ_0, and the pseudo-rigid-body angle, Θ:

$$\theta_0 = c_\theta \Theta \tag{2}$$

where c_θ is the parametric angle coefficient. Now the end deflections a and b can be determined by the kinematics of the rigid link. A compliant system can be modeled with a number of PRBMs.[13]

Yu et al. developed the following theory for modeling dynamic PRBMs denoted PRBDMs.[10] The foundation of this theory is the principle of dynamic equivalence.[21] In the case presented in Fig. 3b, the kinematic parameters and characteristics of the PRBM and PRBDM are the same. In addition, a dynamic spring constant for an end moment, K_d is defined as:

$$K_d = c_\theta K \tag{3}$$

Finally, the end moment can be related to the pseudo-rigid-body angle by:

$$M_0 = K\Theta \tag{4}$$

The PRBDMs presented in Ref.[10] do not model damping explicitly since the model validation was performed on the natural frequencies of the compliant system. Since we are concerned with time domain simulations, the unavoidable damping in the system must be included. We denoted the linear damping constant at the joint as B_d. Additional simulations determined 1 Nms/deg as a reasonable value for this constant.

Other approaches based on PRBMs to model the dynamics of flexible members includes the method proposed by Wang and Yu.[22] Modeling the SA as a single PRBDM does not provide much freedom performing a desired task since only a single moment value can be defined along the member. Therefore, it is desirable to discretize the SA into smaller members allowing for more control over the moment function along the SA. Su demonstrated the utility of three discretized members which would allow for additional control moments.[23] The system variables for the satellite model with 3 PRBDM discretizations per SA (denoted as $n_p = 3$) is presented in Fig. 4. The metallic mounting spring constants would be lumped into the dynamic spring constants of the SA.

II.C. SimMechanics® Model

One method of predicting the dynamic response of the system shown in Fig. 4 is to first obtain the Euler-Lagrange equations of motion with the equivalent kinetic and potential energies easily defined for the PRBDM. With a closed-form solution, either a simulation or simultaneous analysis and design approach

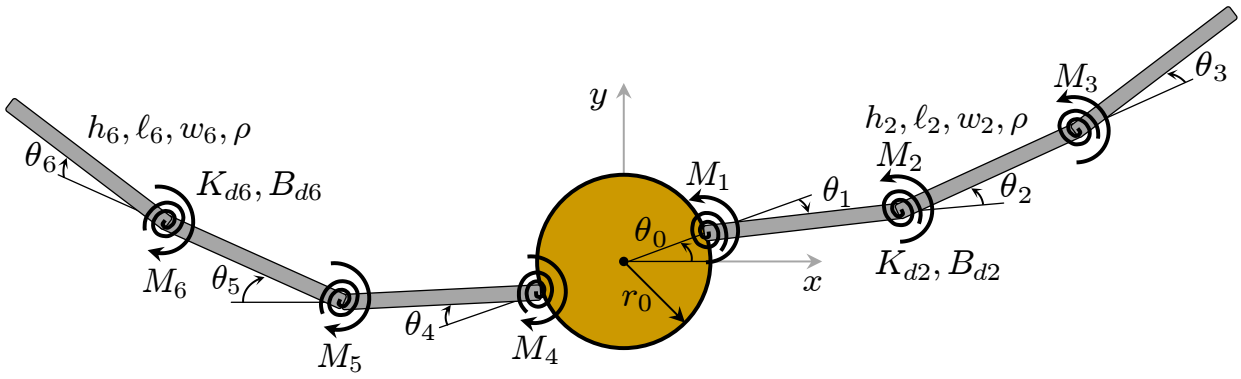

Figure 4: Select system variables for 3 PRBDM discretizations per solar array.

can be used to satisfy the dynamics while optimizing the system. If the equations of motion are challenging to derive, a computational model can be created that will perform the dynamic analysis. One such toolbox suited for multibody simulations of mechanical systems is the SimMechanics® toolbox for use in the Simulink® environment.[24] Using modeling strategy based on SimMechanics® will support the development of substantially more complex system models in the future. In other words, this strategy is more scalable than deriving system equations by hand.

The SimMechanics® model is presented in Fig. 5. There are 3 main subsystems: SB, SA, and control input. The SB subsystem is shown in Fig. 5b. The rigid cylinder's physical properties are based on the system description and the center of the cylinder is connected to a freely rotating revolute joint. Rigid transforms are used to define SA connection ports that are located at either side of the SB. The SB then can be connected to a varying number of SA subsystems and control inputs depending on the level of discretization modeled. The SA subsystem is shown in Fig. 5c. The revolute joint is parameterized by both K_d and B_d that are calculated using the theory from Sec. II.B before each simulation. Rigid transforms are used to translate from the spring to the center to the end of the beam.

The panel is defined using a rectangular prism solid with variable length, width, height, and density. An external moment block functions as an intermediary between the control input signal and the actual moment acting on the SA. This subsystem can easily be 'stringed' together to form the more discretized SA. The control input subsystem is just a PS Lookup Table (1D) block[a] modified with the current simulation time as the independent lookup value (see Ref.[25]). The use of a lookup table implies that we parametrized the control (i.e., we can only directly change a few discrete values and will interpolate the remaining).

II.D. Using Frequency Specifications for the Identification of Physical Properties

The description of the satellite required a bending frequency of 2.5 Hz for the SA. In Eqn. (1), all physical properties of the array have already been specified except the elastic modulus, E. Therefore, to produce the correct natural frequency, the appropriate value for E must be found. A sensitivity study was performed varying the elastic modulus from 10^7 to 10^{10} Pa. Since we are only concerned with the primary frequency, the system was excited with a constant moment (i.e., the input disturbance only needs a single level of excitation to capture this frequency). The fast Fourier transform (FFT) was used to obtain the frequency properties of the time domain simulation, then the power of the discrete Fourier transform was used to identify the dominant frequency.

The results of this study are found in Fig. 6. In Fig. 6a we see the elastic modulus versus identified frequency with the horizontal line indicating 2.5 Hz. The two different discretizations of the SA have different frequency responses for a given value of E since as ℓ decreases, the K_d increases and this ratio of panel lengths is constant for differing values of E. Identified values for E for when $n_p = 1$ was 4.98×10^7 Pa while $E = 2.13 \times 10^7$ Pa when $n_p = 3$, which are both similar to E for low-density polyethylene. The circled dots in Fig. 6a correspond to the normalized periodograms (frequency versus power) in Fig. 6b. We can see a clear dominant frequency and the additional peaks are most likely due to numerical errors commonly encountered when using the FFT algorithm.

[a] `http://www.mathworks.com/help/physmod/simscape/ref/pslookuptable1d.html`

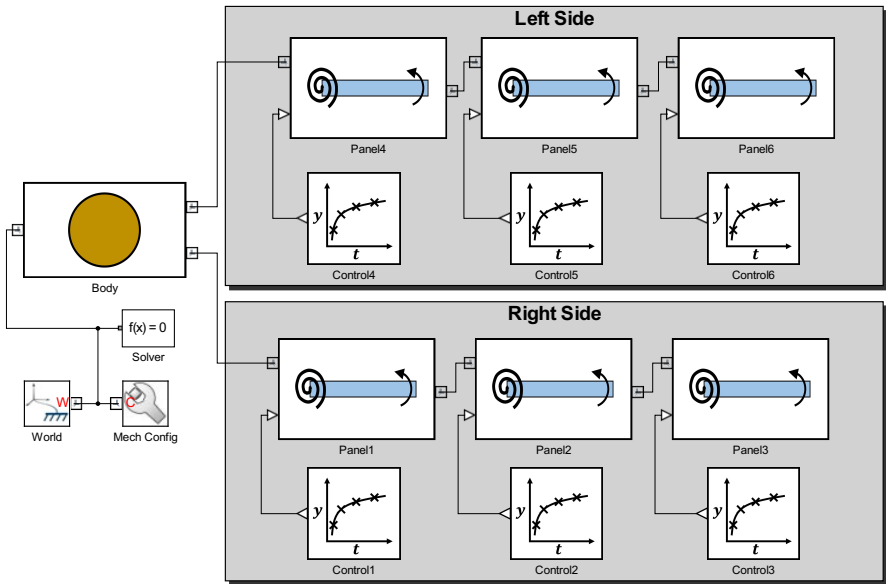

(a) Complete SimMechanics® model with 3 divisions per solar array.

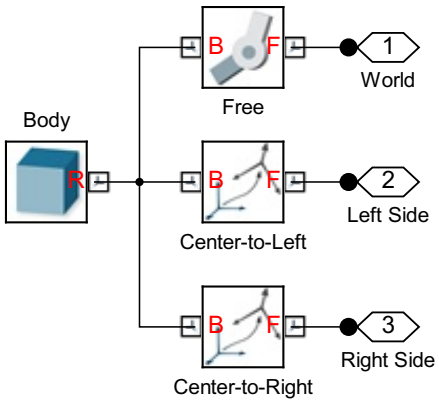

(b) Satellite body subsystem.

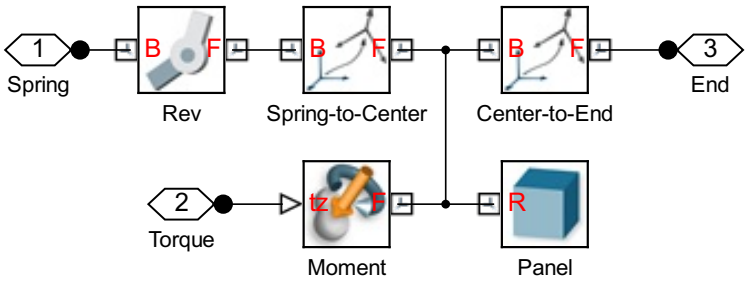

(c) Solar array subsystem.

Figure 5: SimMechanics® model.

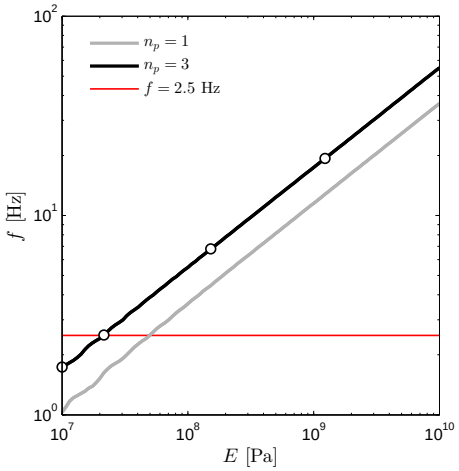

(a) E sensitivity study.

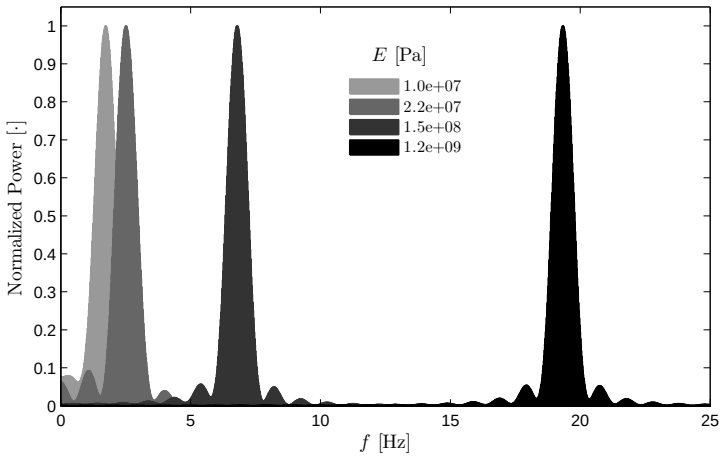

(b) Normalized periodogram for select values of E and $n_p = 3$.

Figure 6: Sensitivity study to determine the elastic modulus that produced the desired SA frequency.

III. Attitude Control Utilizing the Solar Arrays

III.A. Basic Physics Analysis

We start our analysis of the attitude control problem by assuming the entire satellite is a rigid body. This provides a rough point of comparison, and helps to develop basic intuition for the motion of this system. The effective moment of inertia of one SA is calculated by:

$$I_{zz,\mathrm{SA}} = \frac{m_{\mathrm{SA}}}{12}\left(h^2 + \ell^2\right) + m_{\mathrm{SA}} r^2 \tag{5}$$

where $I_{zz,\mathrm{SA}}$ is the moment of inertia about the center of the SB, $m_{\mathrm{SA}} = 20$ kg is the array mass, $h = 0.025$ m is the array height, $\ell = 2$ m is the array length, and r is the 2 m distance between the center of mass of the SA and the center of the SB. The effective moment of inertia of both satellite arrays is 173.3 kgm^2 compared to the 2000 kgm^2 inertia of the body. This means that the arrays are more than 11 times easier to rotate than the SB.

At this point, it is assumed that the control being applied is a torque acting between the SB and SAs at their points of contact. One feasible control trajectory that will accomplish a slewing maneuver in a single rotating plane is linear and symmetric (i.e., the moments applied by each panel is symmetric and varies linearly with time such that the moment at the initial time is the opposite of the moment applied at the final time). The symmetric nature implicitly requires the system to come to rest at the end of the time horizon assuming that it started at rest (i.e., $\dot{\theta}_0(t_0) = \dot{\theta}_0(t_f) = 0$). The linear shape of the control input results in a monotonically increasing θ_0. With these assumptions, along with a specified end time and final angular position, there exists only one feasible linear symmetric control trajectory. Solving for this trajectory produces the following result:

$$M(t) = M_{\max}\left(\frac{2t}{t_f} - 1\right) \tag{6}$$

where $M_{\max}$ is the maximum moment applied, and t_f is the final time value. In the absence of any other forces, the angular acceleration, $\ddot{\theta}_0$, depends on this moment and the inertia of the system: $\ddot{\theta}_0 I_{zz} = M(t)$. Integrating this equation twice yields:

$$\theta_0(t) = \frac{M_{\max}}{I_{zz}}\left(\frac{t^3}{3t_f} - \frac{t^2}{2}\right) + \dot{\theta}_0(t_0)t + \theta_0(t_0) \tag{7}$$

Using this equation, we can determine the value of $M_{\max}$ required to change the attitude of the satellite by angle θ in time t_f. For example, let $t_f = 10$ s, $\theta_0(t_f) = 90^\circ = \pi/2$ radians, $I_{zz} = 2173.3$ kgm^2 (total SC moment of inertia), and assume zero initial conditions. The resulting maximum moment is $M_{\max} = -204.8$ Nm, or 102.4 Nm acting on each solar panel. Hale et al. found similar solutions for a single-axis slew maneuver when only the SB was actuated.[2] This number will be compared to the model response later. We will now discuss how we can move away from the rigid assumptions to a more compliant model of the SAs.

III.B. Optimal Attitude Control

Various objectives have been proposed for satellite attitude control, including time-optimal, fuel-optimal, mass minimization, or a multiobjective combination of performance metrics.[5,8] In our formulation we will seek to minimize the moment functions required, which is analagous to fuel-optimal. The moment functions are ideally defined spatially along the SA as well as temporally. Moment functions will be discretized spatially to permit the use of PRBDMs, and temporally to allow use of direct optimal control. No actuators will be placed on the payload, only the SA. Attitude is measured based on payload orientation. The attitude control will be enforced at simulation boundaries (t_0 and t_f), and jitter will be reduced by requiring the final angular velocities to be near zero at the end of the time horizon. Minimizing jitter at the end of the maneuver helps to increase the rate at which data can be gathered by the camera (payload) after a maneuver. The continuous

reorientation problem is posed as:

$$\min_{\mathbf{M}(t)} \quad \int_{t_0}^{t_f}\int_{0}^{\ell} \|\mathbf{M}(t)\|_2^2 ds dt \tag{8a}$$

$$\text{subject to:} \quad \begin{bmatrix}\boldsymbol{\theta}(t_0)\\ \dot{\boldsymbol{\theta}}(t_0)\end{bmatrix} = \begin{bmatrix}\boldsymbol{\theta}_0\\ \mathbf{0}\end{bmatrix} \tag{8b}$$

$$\begin{bmatrix}\boldsymbol{\theta}(t_f)\\ \dot{\boldsymbol{\theta}}(t_f)\end{bmatrix} = \begin{bmatrix}\boldsymbol{\theta}_f\\ \mathbf{0}\end{bmatrix} \tag{8c}$$

$$\text{where:} \quad \dot{\boldsymbol{\xi}}(t) = \mathbf{f_d}\left(\boldsymbol{\xi}(t), \mathbf{M}, t\right) \tag{8d}$$

where $[t_0, t_f]$ is the time horizon, $\boldsymbol{\xi}(t)$ are the state trajectories, $\mathbf{M}(t)$ are the control moment trajectories, s is the distance along the SA, and $\mathbf{f_d}(\cdot)$ is the time derivative function defined using the SimMechanics® model illustrated in Fig. 5. The nondiscretized objective function is defined in Eqn. (8a). The initial and final value constraints are in Eqns. (8b) and (8c). The dynamics are satisfied implicitly, as expressed in Eqn. (8d), by completing a dynamic simulation for each optimization function evaluation, so are not included as explicit constraints.[26]

The continuous objective in Eqn. (8a) can be approximated using numerical quadrature. The composite trapezoidal rule is used here in temporal discretization, and discretization along the the spatial dimension is performed using a nonweighted sum of the moment function at each panel. Since shooting approaches can have numerical difficulties satisfying boundary conditions, final constraint value tolerances were included. These can be thought of as residual jitter present after the completion of the maneuver. The initial conditions do not require this modification since they are specified at the start of the simulation. With these adjustments, the modified reorientation problem is stated as:

$$\min_{\mathbf{M}} \quad \frac{1}{2}\sum_{p=1}^{2n_p}\sum_{k=1}^{n_t} h_k\left[M_p^2(t_k) + M_p^2(t_{k-1})\right] \tag{9a}$$

$$\text{subject to:} \quad \begin{bmatrix}\theta_0(t_0)\\ \theta_p(t_0)\\ \dot{\theta}_0(t_0)\\ \dot{\theta}_p(t_0)\end{bmatrix} = \begin{bmatrix}0\\0\\0\\0\end{bmatrix} \qquad p = 1, \ldots, n_p \tag{9b}$$

$$\begin{bmatrix}|\theta_0(t_f) - \theta_{0,f}|\\ |\theta_p(t_f)|\\ |\dot{\theta}_0(t_f)|\\ |\dot{\theta}_p(t_f)|\end{bmatrix} \leq \begin{bmatrix}\epsilon_1\\ \epsilon_2\\ \epsilon_3\\ \epsilon_4\end{bmatrix} \qquad p = 1, \ldots, n_p \tag{9c}$$

$$\text{where:} \quad \dot{\boldsymbol{\xi}} = \mathbf{f_d}\left(\boldsymbol{\xi}, \mathbf{M}\right) \tag{9d}$$

where n_t is the number of temporal time steps, $\theta_{0,f}$ is the specified final SB angle, and ϵ are the final value tolerances. We are typically most concerned with accurate final SB states, so these tolerances were made quite small ($\epsilon_1 = 10^{-5}$ rad and $\epsilon_3 = 10^{-2}$ rad/s). The tolerances on the SAs were set to be $\epsilon_2 = 1$ rad and $\epsilon_4 = 1$ rad/s. It was assumed that the residual values would be removed with the jitter reduction strategy. The specific maneuver explored was a reorientation to $\theta_{0,f} = 90°$. The ideal initial and final configurations are shown in Figs. 7a and 7b. An undesirable configuration is shown in Fig. 7c where the maneuver has not been completed and the SA angles are far away from their equilibrium position.

As discussed in the Basic Physics Analysis section, a valid solution to the rigid reorientation problem is linear, symmetric control. Initial implementations allowed for a completely free open-loop control trajectory, but the resulting solutions were tending towards the linear, symmetric control. Therefore, each control function parameterization was reduced to a single quantity, the minimum moment value and linear, symmetric control was assumed in the optimization formulation. This assumption severely limits the set of feasible control values since the basic physics analysis showed that only a single linear control trajectory will satisfy the end boundary conditions. However, using multiple moments on different panels does provide some design freedom (i.e., increasing n_p). In addition, the tolerances do provide some freedom to account for damping and oscillations in the system.

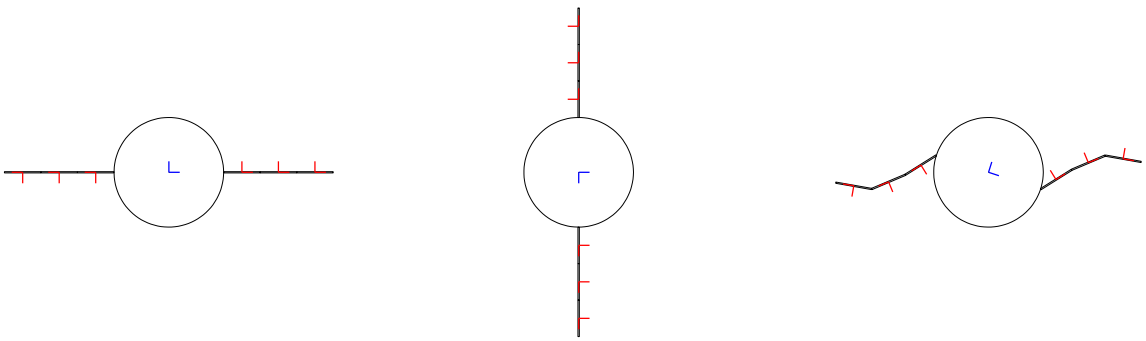

(a) Initial configuration. **(b) Final configuration.** **(c) Potential configuration.**

Figure 7: Various configurations of the satellite reorientation problem.

The results for both 1 and 3 discretization panels per SA are shown in Fig. 8. In both cases we see that the reorientation from 0° to 90° was accomplished within the tight tolerance set. The angular velocity of the body was mostly symmetric, but the initial transient effects of the SAs can be seen at the beginning of the maneuver. The SAs are oscillating about a linear, symmetric line similar to the control values but the initial transient response from the initial equilibrium position creates large initial oscillations. After the transience has subsided, the system is close to a rigid system in a different equilibrium position. Also recall that since the problem is symmetric about the z-axis, the left and right side state trajectories are identical. Finally, the natural frequency of the of SAs is 2.5 Hz as predicted by Fig. 6.

The main difference between the solutions is the final control values. With $n_p = 1$, $M_{\max} = 102.373$ Nm and for $n_p = 3$, $\mathbf{M}_{\max} = [34.013 \text{ Nm}, 34.687 \text{ Nm}, 33.669 \text{ Nm}]$. Each maximum moment in the three-panel case is much smaller, and since the moments are squared in the objective function, the final cost is much lower (i.e., 23,310 compared to 69,923). A quick sum of these three moments results in 102.369 Nm, which implies the overall moment on the system is nearly the same in both models and is nearly the same as the basic physics analysis on the rigid system. Increasing the number of actuators results in smaller control cost per actuator.

SA oscillation magnitude for the 3 panel model decreased with distance from the SB. This is due to the coupling between the SAs. The magnitude of oscillation of the spring connected to the SB was smaller in the 3 panel model most likely due to the smaller control moments. In the next section we will discuss how the system responds to jitter from the slewing maneuver and an internal disturbance.

IV. Jitter Reduction Utilizing the Solar Arrays

This section will focus on the passive response of the system subject to a number of unstable scenarios. The vibrations or jitter may also occur in individual components of the SB but for now, they are all grouped into the rigid SB. Active control may be used (and will mostly likely be needed in a fully-developed system) but utilizing the passive dynamics is critical in challenging co-design problems. The crucial element that removes energy from the system is dynamic damping, characterized by the constant B_d. In the same sense that actuators must be selected for attitude control, damping components will also need to be identified.

IV.A. Post-Slew Maneuver Response

At the end of the slewing maneuvers presented in Fig. 8, the SA moments are non-zero, and as a result the angular positions of each panel is also non-zero. This result is congruent with conservation of angular momentum. If the SC starts of at rest, it has zero angular momentum. To change the SB orientation without external forces (e.g., thrusters or Earth magnetic field reactions) or reaction wheels, the relative orientation of the SA must be different in the final state.

The slew maneuver induces vibration in the system, as illustrated in Fig. 8. This is one of several potential sources of jitter. To observe this post-slew maneuver behavior, the simulation was continued

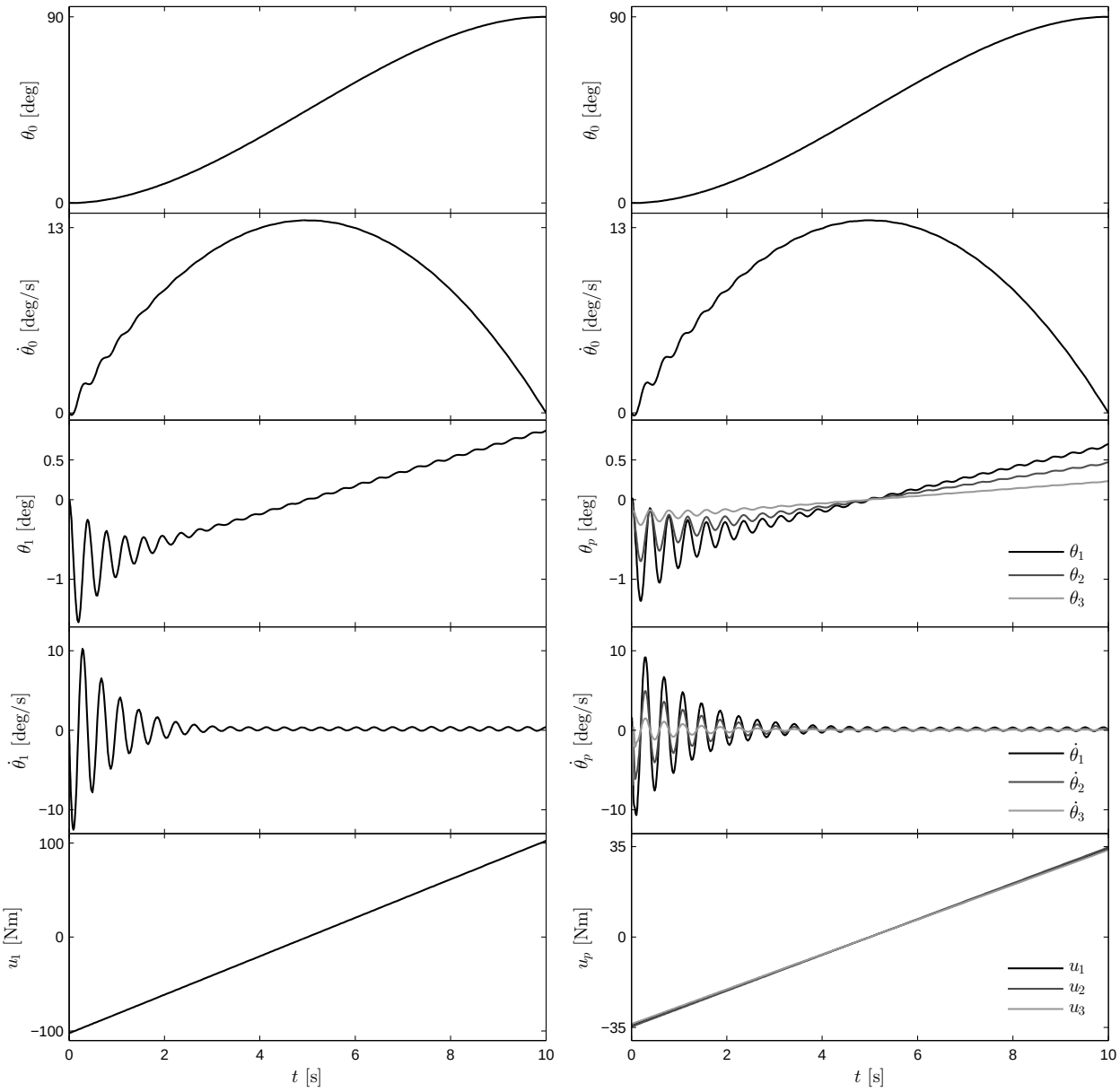

(a) $n_p = 1$. **(b)** $n_p = 3$.

Figure 8: State and control trajectories with linear, symmetric optimal control.

beyond $t_f = 10$ s with an instantaneous removal of the control moments. The result is illustrated in Fig. 9a. This figure demonstrates the coupling between the SB and the SAs quite well since the momentum is transferred quickly between them at the natural frequency of the SAs. Some of the energy transferred to the SAs can be dissipated with damping, as illustrated by the decay of the response.

At $t_0 = 0$ seconds, velocities are zero, so total momentum is zero. Due to conservation of momentum, the total momentum of the system must remain zero. At $t_f = 10$ seconds the SB and SA velocities are non-zero. The SA momentum cancels out SB momentum, so the total system momentum is still zero. Before data can be gathered by the camera the SB must be in its desired orientation with zero angular velocity. In the current simulation at t_f the SB orientation is correct, but its velocity is non-zero. Achieving the desired SB orientation with zero velocity would require a different control strategy that gradually reduces SA control moments as t_f is approached such that at t_f the elastic forces pushing the SA back to its equilibrium position

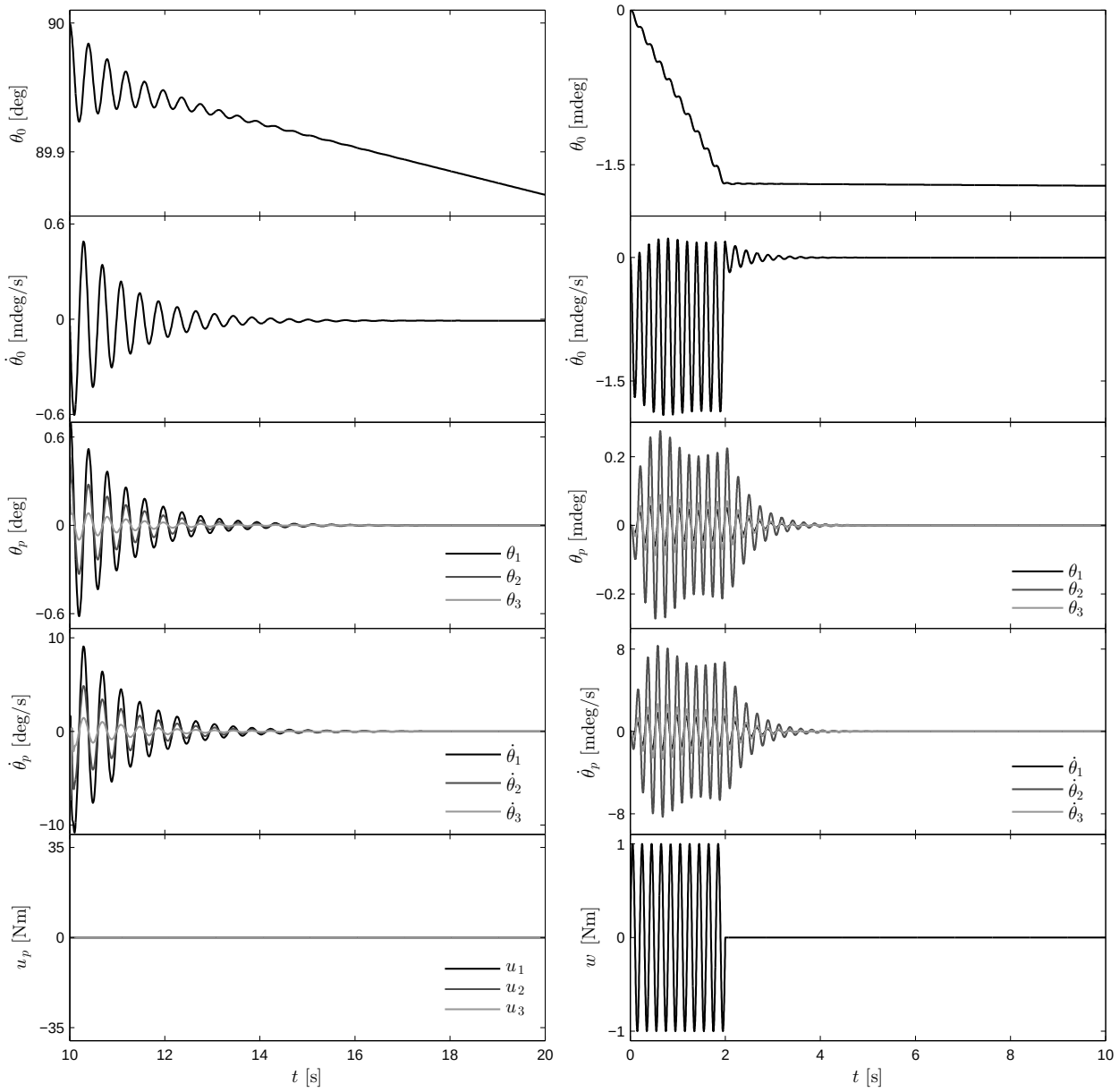

(a) Post-slew maneuver response. **(b) Short-term internal disturbance response.**

Figure 9: State, control, and disturbance trajectories for 2 jitter studies.

are exactly balanced. The SA must maintain its deformed position to keep the SB at its new orientation; simply releasing the SA (i.e., setting control moments to zero) would cause the SB and SA orientations to move back to their original orientations at t_0.

IV.B. Short-Term Internal Disturbances

Other internal components, such as reaction wheels or gimbaled payloads, can produce unwanted disturbances. To observe the system's response to this type of disturbance a sinusoidal moment was applied to the an initially stable SB. This disturbance took the form: $w = \sin(10\pi t)$ Nm, and was applied for 2 seconds. The results of the experiment are in Fig. 9b.

During the first 2 s, the oscillations in the SB propagate outwards towards the SAs. Based on the nature of the disturbance (i.e., it is modeled as an external force), θ_0 performs a relatively large rotation during this

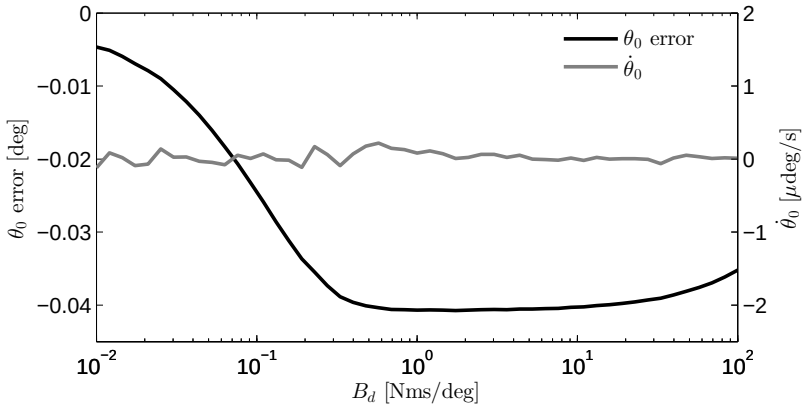

Figure 10: Long-term reorientation error and SB velocity sensitivity to B_d.

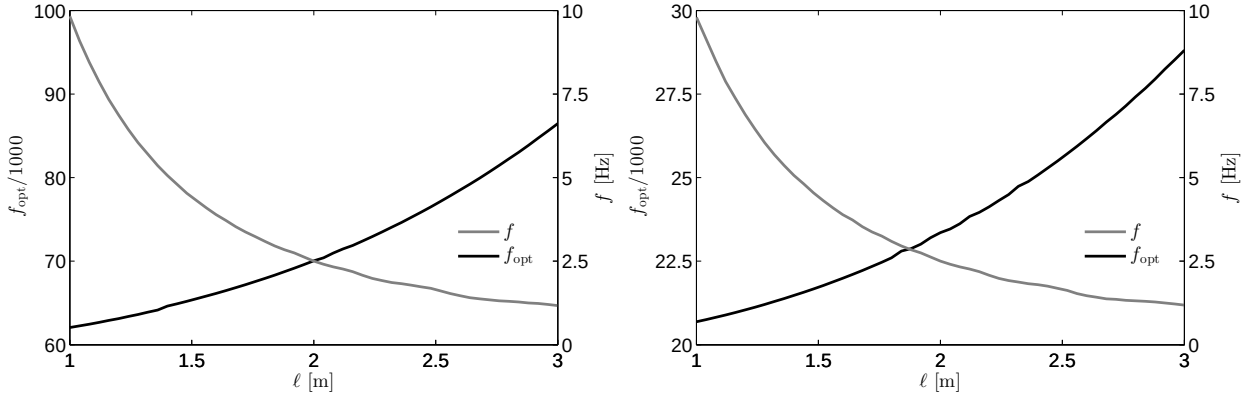

(a) $n_p = 1$. **(b) $n_p = 3$.**

Figure 11: Objective function and bending frequency sensitivity to ℓ.

initial window. Once the disturbance is removed, the system decays similar to the behavior in Fig. 9a. Once again the angular velocity of the SB is nonzero even after a large period. This again causes constant drift. However when compared to the results of the rigid system under the same disturbance, the flexible system with damping has a smaller drift value. This is because some of the energy from the input is dissipated by the SAs, while no such mechanism exists in the rigid system. In this scenario it favorable for energy to flow to the SAs, potentially contrary to conventional design procedures.

IV.C. Physical Design Sensitivities

The selected value of $B_d = 1$ Nms/deg was not based on a real system, but rather was identified by selecting a value that matched the expected dynamic behavior. To better understand the effect of this damping coefficient on both the attitude control results and jitter reduction, a sensitivity study was performed. The first stage of this study required a solution to Prob. (9) (i.e., linear, symmetric control found using shooting). The next stage was the post-slew maneuver response but for an extended period of time (1000 s) in order to observe the final steady state behavior. Then the long-term final values of θ_0 and $\dot{\theta}_0$ were recorded. The long-term value for θ_0 indicates how much error is expected due to the boundary constraint tolerances. The angular velocity indicates the magnitude of any additional drift that may occur after 1000 s.

In Fig. 10, we observed that small values of damping have smaller errors. This might be counterintuitive since low damping in a flexible system results in high oscillations. While this is also true for this system, these oscillations tend to be highly symmetric about the equilibrium position. Higher values of damping are more asymmetric since a larger portion of energy is taken out during each cycle; hence successive cycles are quite different. The slight decrease in error at extreme values of damping are due to the system being

overdamped. The long-term values of $\dot{\theta}_0$ were nonzero as seen in the other jitter responses. Even with extremely high values of damping, the response will only be asymptotically decaying. Given enough time, even lightly damped systems will decay.

We now transition to a final physical design study. As previously mentioned, it is imperative to consider how the physical system is coupled with the control. Increasing ℓ results in heavier panels with more inertia. Therefore, the maximum moment found in Eqn. (7) will have to increase. On the other hand, examining Eqn. (1), decreasing the length should increase the value of K. This implies the frequency of the panel increases. To verify this relationship, a sensitivity study varying the length of the SA was performed. All other properties of the SAs were held constant including the value of E found in Fig. 6a. This results of this study are presented in Fig. 11. As expected, as ℓ increases, the objective function value increases while the natural frequency of the SA decreases. Note that the range values of f is quite large between 1.5 and 10 Hz. The control effort range is smaller since at even large values of ℓ, the inertia of the SA is smaller than the inertia of the SB. If a specific frequency of the SA is more desirable, it can be tuned efficiently related to the additional control effort. This study poses a design trade-off between control effort required to reorient the satellite versus expected jitter frequency at the end of the maneuver.

V. Future Design Considerations

This section will discuss a few additional elements of the design problem that need to be considered to produce more useful solutions.

V.A. Co-Design with Direct Transcription

Shooting methods are straightforward to include in optimization formulations since they can use conventional differential algebraic equation solvers and traditional modeling paradigms. However, there are a number of numerical issues to consider. For each perturbation in the optimization algorithm, a full simulation needs to be performed and convergence is not guaranteed for open-loop unstable systems.[16,26] Many of the convergence issues are due to the inability to efficiently handle path and boundary constraints (see Ref.[25] for a numerical example).

An alternative direct method of optimal control is direct transcription (DT). This approach includes both the states and control as optimization variables. As a consequence of this fact, DT will avoid nested simulation by including the dynamic collocation equations directly as optimization constraints. While this results in a large dimension optimization problem, its structure can be exploited for efficient solution.[16,26] Now boundary and inequality path constraints may be imposed directly on states, control inputs, physical system design variables, or functions of these quantities avoiding many of the issues encountered in a shooting approach.

DT has been used to solve a number of attitude control problems particularly for time-optimal satellite maneuvers.[16,19,27,28] Recently, DT has been extended for a variety of co-design problems including automotive suspensions[29] and wave energy converters.[17] Problems formulated with DT can easily include time-independent parameters, enabling efficient solution of co-design problems.[29] Recent work by Herber has shown that DT formulation can use a SIMSCAPE® model (similar to SIMMECHANICS® model) for the state derivatives of the system.[25] Thus it might be possible to directly include the model in Fig. 5 in a DT formulation.

V.B. Open-Loop Design as an Early-Stage Design Tool

In a true open-loop design problem (i.e., no feedback or forced parameterizations of the control such as requiring it to be linear and symmetric), no assumptions on the control structure are imposed. This approach may prove especially helpful during early-stage design when the control architecture is undefined and the optimal controller may not exist in the current state-of-the-art. In addition, open-loop solutions can provide insights into upper system performance limits without the restrictions imposed by specific physical- and/or control-system design.[4] Without knowing the true upper performance limits of the compliant system, we will not know how close we are to a truly optimal system design.

The open-loop solutions can also provide possible directions for physical-system design, such as which actuators can closely match the optimal open-loop trajectories (e.g., can reaction wheels or embedded piezoelectric wafers produce these control trajectories effectively?)[4,17] In addition, the open-loop solutions can

also provide insights into complex system dynamics, and serve as a basis for developing implementable feedback control systems.[30,31] Only with more advanced solution procedures such as co-design with DT can we pursue a true system-level optimization formulation and potentially identify the desired novel physical- and/or control-system designs.

V.C. Realistic Compliant Dynamic System Models

Design of compliant mechanisms for a prescribed dynamic behavior are not well studied. While PRBMs are accurate modeling and analysis tools for static and dynamic behavior, obtaining practical geometries that result from system parameters require new design guidelines. Furthermore a PRBM typically considers an end load or a single moment acting on the member.[13] However, the system described in Fig. 4 requires a number of discrete moments along the SA. Simply linking a number of cantilever beam PRBDMs subject to an end moment may not accurately model the system. Su demonstrated that a cantilever beam can be divided into 3 sections and accurately predict the kinematics for large deflections but the ideal characteristic radius factors (γ) were not all the same.[23] His modeling objectives differ from ours since we are concerned with the dynamics of the individual segments, moments applied to each segment (not just the end), and smaller deflections.

New high-fidelity models need to be developed to verify that our approach is valid or if certain system parameters such as γ need to be updated. This model will be created with the physical system in mind, i.e., it should depend on the independent design variables such as the SA's geometric properties. This will provide a simple mapping between the lumped parameters used in the PRBDMs and the realistic design variables.

The higher-fidelity model is not meant to replace the PRBDMs or SimMechanics® model but aid in accurate model creation. Since PRBDMs decouple the kinematics and elastic behavior, it is a computationally inexpensive approach that is more suitable for design. Through experiments on the higher-fidelity model, surrogate models may be constructed instead of the Eqns. (1)–(4) that more accurately map the physical system design to the PRBDM parameters (e.g., $K = f(\gamma, K_\theta, E, I, \ell)$). Finally, a space mapping approach could be utilized to produce both accurate and computationally inexpensive models.[32] This approach aligns a fast coarse model (SimMechanics® model based on PRBDMs) with the expensive-to-compute accurate model.

One candidate for the high-fidelity model is to use nonlinear finite elements.[11,12] Another approach is subspace identification of a specific SA.[33] Co-design can be challenging to perform with system identification approaches since there is not a direct mapping to the independent design variables. However, these models can be useful if we are designing the controller for an already fabricated structure.

VI. Conclusion

Solar arrays are a necessary component of many SC systems. These are large, flexible structures that are typically designed in a decoupled manner from the main satellite body. Integrating the compliance of the SAs into the system model produces additional dynamics, and through an intelligent design process, these dynamics may be favorable for a mission. In this article, we used a PRBDM approach to create a lumped compliance model that is favorable for analysis and co-design studies. With specified frequency properties of the SAs, the elastic modulus was identified that produced the desired behavior.

Attitude control was accomplished through external linear, symmetric moments acting on the SAs. Increasing the number of actuators (and therefore the number of solar array discretizations) reduced the maximum required moment in each actuator. The passive dynamics of the system were observed for a number of jitter conditions. This included post-slew maneuver response, short-term internal disturbance response, and the sensitivity of the long-term slewing error as a function of internal damping. The effect of the SA length on both the required control and frequency properties of the SA was identified.

A number of future design considerations are planned, including co-design studies using direct transcription and developing accurate compliant dynamic system models that are better suited for realistic system design. Future work will include updating the models used in these studies to use internal control moments instead of external. Updating the models in this way will introduce additional limitations in system performance (e.g. the range of angles which the SB can be reliably rotated by the SA dynamics, the power required to initiate a movement and maintain a position, etc.). These limitations should be explored to give

a realistic view of the range of effective control using this approach. The models will further be updated to more realistically model the jitter caused by reaction wheels and reorientation of scientific tools.

References

[1]Agrawal, B., "Jitter Control for Imaging Spacecraft," *IEEE/ASTIN 2009 International Conference on Recent Advances in Space Technologies*, June 2009, pp. 615–620.

[2]Hale, A. L., Lisowski, R. J., and Dahl, W. E., "Optimal Simultaneous Structural and Control Design of Maneuvering Flexible Spacecraft," *AIAA Journal of Guidance, Control, and Dynamics*, Vol. 8, No. 1, Jan. 1985, pp. 86–93.

[3]Fonseca, I. M. and Bainum, P. M., "Large Space Structure Integrated Structural and Control Optimization, Using Analytical Sensitivity Analysis," *AIAA Journal of Guidance, Control, and Dynamics*, Vol. 24, No. 5, Sept.–Oct. 2001, pp. 978–982.

[4]Allison, J. and Herber, D., "Multidisciplinary Design Optimization of Dynamic Engineering Systems," *AIAA Journal*, Vol. 52, No. 4, April 2014, pp. 691–710.

[5]Zhang, S., Qian, S., and Zhan, L., "Chapter 23: Optimal Control Techniques for Spacecraft Attitude Maneuvers," *Advances in Spacecraft Technologies*, edited by J. Hall, InTech, 2011, pp. 523–548.

[6]Bodineau, G., "(μ-Mu)-iteration Technique Applied to the Control of Satellites with Large Flexible Appendages," *ESA 2005 International Conference on Guidance, Navigation & Control Systems*, Oct. 2005, pp. 583–592.

[7]Loquen, T., "Attitude Control of Satellites with Flexible Appendages: A Structured $\mathcal{H}_\infty$ Control Design," *AIAA Guidance, Navigation, and Control Conference*, Aug. 2012.

[8]Toglia, C., "Optimal Co-design for Earth Observation Satellites with Flexible Appendages," *AIAA Guidance, Navigation, and Control (GNC) Conference*, Aug. 2013.

[9]Alazard, D., "Linear Dynamic Modeling of Spacecraft with Various Flexible Appendages and On-board Angular Momentums," *ESA 2008 International Conference on Guidance, Navigation & Control Systems*, June 2008.

[10]Y-Q, Y., Howell, L. L., Lusk, C., Yue, Y., and He, M.-G., "Dynamic Modeling of Compliant Mechanisms Based on the Pseudo-Rigid-Body Model," *ASME Journal of Mechanical Design*, Vol. 127, No. 4, Jul. 2005, pp. 760–765.

[11]Robinett, R., Dohrmann, C., Eisler, G., Feddema, J., Parker, G., Wilson, D., and Stokes, D., *Flexible Robot Dynamics and Controls*, Kluwer Academic/Plenum Publishers, 1st ed., 2002.

[12]Eisler, G., Robinett, R., Segalman, D., and Feddema, J., "Approximate Optimal Trajectories for Flexible-Link Manipulator Slewing Using Recursive Quadratic Programming," *ASME Journal of Dynamic Systems, Measurement, and Control*, Vol. 115, No. 3, Sept. 1993, pp. 405–410.

[13]Howell, L. L., Magleby, S. P., and Olsen, B. M., *Handbook of Compliant Mechanisms*, Wiley, 1st ed., 2013.

[14]Knot, N. S., "Structure/Control Optimization to Improve the Dynamic Response of Space Structures," *Springer Computational Mechanics*, Vol. 3, No. 3, May 1988, pp. 179–186.

[15]Sunar, S. and Rao, S. S., "Simultaneous Passive and Active Control Design of Structures Using Multiobjective Optimization Strategies," *Elsevier Computers & Structures*, Vol. 48, No. 5, Sept. 1993, pp. 913–924.

[16]Betts, J. T., *Practical Methods for Optimal Control and Estimation Using Nonlinear Programming*, SIAM, 2nd ed., 2009.

[17]Herber, D. R. and Allison, J. T., "Wave Energy Extraction Maximization in Irregular Ocean Waves using Pseudospectral Methods," *ASME 2013 International Design Engineering Technical Conferences*, No. DETC2013-12600, Aug. 2013.

[18]Ross, I. M., Sekhavat, P., Fleming, A., and Gong, Q., "Optimal Feedback Control: Foundations, Examples, and Experimental Results for a New Approach," *Journal of Guidance, Control, and Dynamics*, Vol. 31, No. 2, 2008, pp. 307–321.

[19]Melton, R. G., "Numerical Analysis of Constrained, Time-Optimal Satellite Reorientation," *Hindawi Mathematical Problems in Engineering*, Vol. 2012, 2012, Article ID 769376.

[20]Deshmukh, A. and Allison, J. T., "Design of Nonlinear Dynamic Systems using Surrogate Models of Derivative Functions," *ASME 2013 International Design Engineering Technical Conferences*, No. DETC2013-12262, Aug. 2013.

[21]Erdman, A. and Sandor, G., *Mechanism Design: Analysis and Synthesis*, Prentice Hall, 3rd ed., 1997.

[22]Wang, W. and Yu, Y., "Dynamic Modeling of Compliant Mechanisms Based on the Pseudo-Rigid-Body Model," *ASME Journal of Mechanisms and Robotics*, Vol. 2, No. 2, Apr. 2010, pp. 021003.

[23]Su, H., "A Pseudorigid-Body 3R Model for Detmining Large Deflection of Cantilever Beams Subject to Tip Loads," *ASME Journal of Mechanisms and Robotics*, Vol. 1, No. 2, May 2009, pp. 021008.

[24]"SimMechanics: Model and Simulate Multibody Mechanical Systems," Website, `http://www.mathworks.com/products/simmechanics/`.

[25]Herber, D. R., "Solving Optimal Control Problems using Simscape Models for State Derivatives," Tech. Rep. UIUC-ESDL-2014-01, Engineering System Design Lab, June 2014.

[26]Herber, D. R., *Dynamic System Design Optimization of Wave Energy Converters Utilizing Direct Transcription*, M.S. Thesis, University of Illinois at Urbana-Champaign, May 2014.

[27]Izzo, D., Bevilacqua, R., and Valente, C., "Optimal Large Reorientation Manoeuvre of a Spinning Gyrostat," *Cranfield 2004 Conference on Dynamics and Control of Systems and Structures in Space*, Jul. 2004, pp. 607–616.

[28]Yutko, B. M. and Melton, R. G., "Optimizing Spacecraft Reorientation Maneuvers Using a Pseudospectral Method," *Journal of Aerospace Engineering, Sciences and Applications*, Vol. 2, No. 1, Jan.-Apr. 2010, pp. 1–14.

[29]Allison, J. T., Guo, T., and Han, Z., "Co-design of an Active Suspension using Simultaneous Dynamic Optimization," *ASME Journal of Mechanical Design*, Vol. 136, No. 8, Aug. 2014, pp. 081003.

[30]Schaal, S. and Atkeson, C. G., "Open Loop Stable Control Strategies for Robot Juggling," *IEEE 1993 International Conference on Robotics and Automation*, May 1993, pp. 913–918.

[31]Mourik, S. v., Zwart, H., and Keesman, K. J., "Integrated Open Loop Control and Design of a Food Storage Room," *Elsevier Biosystems Engineering*, Vol. 104, No. 4, 2009, pp. 493–502.

[32]Koziel, S., Cheng, Q. S., and Bandler, J. W., "Space Mapping," *IEEE Microwave Magazine*, Vol. 9, No. 6, Dec. 2008, pp. 105–122.

[33]Cavallo, A., de Maria, G., and Natale, C. ; Pirozzi, S., "Gray-Box Identification of Continuous-Time Models of Flexible Structures," *IEEE Transactions on Control Systems Technology*, Vol. 15, No. 5, Sept. 2007, pp. 967–981.